Synthesis and Characterization of Poly(methyl methacrylate–butyl acrylate–acrylic acid)/Polyaniline Core–Shell Nanoparticles in Miniemulsion Media

Xiaokuai Xu, Yuanchang Shi, Libo Sun

College of Material Science and Engineering, Shandong University, Jinan 250061, People's Republic of China

Received 5 August 2010; accepted 21 October 2010
DOI 10.1002/app.33647
Published online 16 August 2011 in Wiley Online Library (wileyonlinelibrary.com).

ABSTRACT: Conductive polymer particles, polyaniline (PANI)-coated poly(methyl methacrylate–butyl acrylate–acrylic acid) [P(MMA–BA–AA)] nanoparticles, were prepared. The P(MMA–BA–AA)/PANI core–shell complex particles were synthesized with a two-step miniemulsion polymerization method with P(MMA–BA–AA) as the core and PANI as the shell. The first step was to prepare the P(MMA–BA–AA) latex particles as the core via miniemulsion polymerization and then to prepare the P(MMA–BA–AA)/PANI core–shell particles. The aniline monomer was added to the mixture of water and core nanoparticles. The aniline monomer could be attracted near the outer surface of the core particles. The polymerization of aniline was started under the action of ammonium persulfate (APS). The final product was the desired core–shell nanoparticles. The morphology of the P(MMA–BA–AA) and P(MMA–BA–AA)/PANI particles was characterized with transmission electron microscopy. The core–shell structure of the P(MMA–BA–AA)/PANI composites was further determined by Fourier transform spectroscopy and ultraviolet–visible measurements. The conductive flakes made from the core–shell latexes were prepared, and the electrical conductivities of the flakes were studied. The highest conductivity of the P(MMA–BA–AA)/PANI pellets was 2.05 S/cm.
 J Appl Polym Sci 123: 1401–1406, 2012

Key words: conducting polymers; core–shell polymers; emulsion polymerization

INTRODUCTION

Polyaniline (PANI), an inherently conducting polymer, has attracted considerable attention because of its ease of preparation and environmental stability. PANI is unique among inherently conducting polymers in that its conductivity can be reversibly controlled either electrochemically or chemically. Potential applications of PANI include electrostatic dissipation, anticorrosion coatings, actives delivery, batteries, and solar control.[1–6] However, PANI is nearly insoluble and has poor processability; this is due to its rigid, conjugated double-bond backbone. This has led to scientists exploring PANI composites with thermoplastic polymers. For example, Shin et al.[7] prepared poly(sulfonated *N*-hydroxyethyl aniline)–PANI–poly(sulfonated *N*-hydroxyethyl aniline)–polystyrene (PS) multicore–shell composite particles by chemical oxidation polymerization. Cho et al.[8] synthesized surface-conductive particles consisting of a poly(methyl methacrylate) (PMMA) core and a PANI-coated shell. Their results show that the PANI/PMMA composite particles possessed a higher dielectric constant and conductivity than the pure PANI particle. Ruckenstein and Yang[9] obtained PANI/PS conducting material using an oxidative polymerization method, in which an sodium dodecylsulfate (LAS) aqueous solution was used as a continuous phase and a benzene solution containing aniline and PS was used as a disperse phase. Okubo et al.[10] synthesized PS/PANI composite particles by the chemical oxidative seeded dispersion polymerization of aniline at a temperature of 0°C with monodispersed PS seed particles in an HCl aqueous solution, in which the pH value was kept at 2.5 with a pH stat. The synthesized composite particles had a conductivity of 3.4×10^{-3} S/cm. Liu et al.[11] synthesized core–shell structured semiconducting PMMA/PANI snowmanlike particles and examined their electrorheological characteristics under an applied electric field. Kim et al.[12] synthesized dodecylbenzene sulfonic acid doped PANI particles by emulsion polymerization and studied the electrorheological properties of dodecylbenzene sulfonic acid doped PANI particles dispersed in silicone oil under different operating temperatures and an applied electric field.

In recent years, miniemulsion polymerization and microemulsion polymerization have been used to prepare polymer nanoparticles. Microemulsions[13] consist of spontaneously formed droplets that are less than 100 nm in diameter but generally require high

Correspondence to: Y. Shi (yuanchangshi@sdu.edu.cn).
Contract grant sponsor: Natural Science Foundation of Shandong Province; contract grant number: Y2008C132.

concentrations of surfactant and costabilizer in addition to relatively low solid contents. Miniemulsion polymerization[14–18] is a modified emulsion polymerization process. The used amounts of surfactant and costabilizer are lower than those of microemulsion polymerization. Miniemulsions consist of stable nanometer-sized droplets, and the particle formation in the polymerization of such systems is by droplet nucleation. That is, all of the surfactants are used to stabilize the droplets, and no more micelles are present in the system. Because of these advantages, miniemulsion polymerization has played an important role in making nanometer-size copolymer latexes with unique or improved properties.

In our previous study, we examined the microemulsion copolymerization of styrene and acrylonitrile[19] and successfully prepared PANI-coated poly (styrene-*co*-styrene sulfonate) nanoparticles in a microemulsion system.[20] However, the PS core had a high glass-transition temperature, and its film-forming properties were poor. A polymer with a lower glass-transition temperature can facilitate film formation and improve the processability of core–shell composite particles. It is well known that the glass-transition temperature of poly(methyl methacrylate–butyl acrylate–acrylic acid) [P(MMA–BA–AA)] can be controlled by the monomer ratio. Here, methyl methacrylate (MMA) is a hard monomer, and butyl acrylate (BA) is a soft monomer. Acrylic acid (AA) can introduce acid functional groups: carboxyl groups, which can enhance the interaction between the P(MMA–BA–AA) core and the PANI shell. So in this study, P(MMA–BA–AA) nanoparticles with diameters of 50–70 nm were prepared as the core in a miniemulsion system, and then, PANI-coated P(MMA–BA–AA) nanocomposite particles were prepared by *in situ* oxidative polymerization.

EXPERIMENTAL

Materials and equipment

The water used here was redistilled and deionized. MMA, BA, and AA were distilled at low pressure before polymerization. All other chemicals were analytical grade and were used without further purification. Samples were analyzed with a transmission electron microscope (JEM-100CX, Japan), a Fourier transform infrared (FTIR) spectrometer (Bruck Vector22, Germany), and a Hall effect testing instrument (HMS-3000, Germany).

Synthesis

Synthesis of the P(MAA–BA–AA) latex

MMA (12 g), BA (1 g), and AA (1 g) were mixed with hydrophobe (0.3 g) and were then added to an aqueous solution containing 0.75 g of sodium dodecyl sulfate and 75 g of water. After the mixture was violently stirred for 1 h, miniemulsification was achieved by the ultrasonication of the mixture for 10 min with a Branson sonifier W450 Digital at 90% amplitude. To prevent polymerization due to heating, the mixture was cooled in an ice bath during homogenization.

TABLE I
Reaction Recipes

Sample	P(MMA–BA–AA) miniemulsion	Aniline (μL)	APS (g)
1	2 g	50	0.05
2	2 g	100	0.10
3	2 g	200	0.20
4	2 g	300	0.30

The time between miniemulsification and initiation was minimized to 5 min to reduce the droplet degradation (Ostwald ripening) period. Rapid nucleation was produced with a redox initiator system consisting of sodium bisulfite (0.3 wt % on the basis of the monomer) and ammonium persulfate (0.2 wt % on the basis of the monomer). The polymerization temperature was 65°C. The polymerization was allowed to proceed for 3 h with vigorous stirring at 400 rpm before cooling to room temperature.

Preparation of the PANI-coated P(MMA–BA–AA) latex

The P(MMA–BA–AA) latex (2.0 g) was diluted with 40 mL of distilled water in a 100-mL, three-mouthed, round-bottom flask. The mixture was stirred for 1 h and sonicated for 0.5 h. At the same time, 0.20 mL of HCl (36 wt %) and different amounts of aniline monomer were added to 30 mL of distilled water. The aniline solution was stirred for 1 h and then added dropwise into the previous diluted latex. The mixture was stirred for 4 h before the aqueous solution containing 10 mL of distilled water, and a certain amount of ammonium persulfate ($(NH_4)_2S_2O_8$, APS) was added dropwise to start the polymerization. Finally, the reaction was processed in an ice-water bath with the protection of nitrogen for 24 h to ensure complete polymerization. During this process, continuous, medium-speed stirring was indispensable.

The reaction recipes are summarized in Table I.

Purification

For the purification of the previous P(MMA–BA–AA) composite, excessive acetone was added to the P(MMA–BA–AA) latexes to destroy the miniemulsion system. The P(MMA–BA–AA) latexes were further centrifuged at 8000 rpm, and the supernatant was removed. The precipitates were washed with water and ethanol. The centrifugation, decantation, and redispersion cycle was repeated until the supernatant became transparent. Finally, the P(MMA–BA–AA)

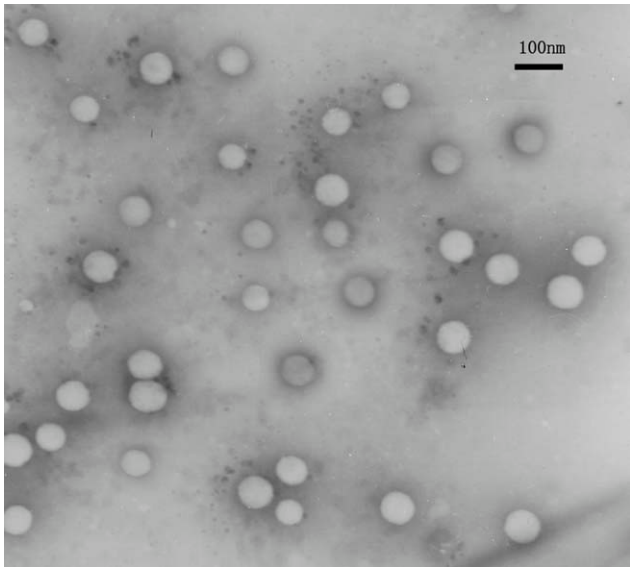

Figure 1 TEM image of the P(MMA–BA–AA) miniemulsion latexes.

nanoparticles were dried in a vacuum oven at 50°C for 12 h. In addition, the purification procedure of the P(MMA–BA–AA)/PANI complex particles was the same as that of the P(MMA–BA–AA) nanoparticles.

RESULTS AND DISCUSSION

Characterization and analysis of the P(MMA–BA–AA) nanoparticles

Transmission electron microscopy (TEM) analysis of P(MMA–BA–AA)

The particle size and morphology were investigated by TEM. For the TEM observations, the P(MMA–BA–AA) latexes were first sonicated, and the samples were prepared by the dropping of highly diluted latexes onto the carbon coated copper grid and were dried in a desiccator at room temperature. The TEM image of the P(MMA–BA–AA) core particles is shown in Figure 1. As shown in Figure 1, the boundary of the particles was distinct and smooth. The diameter of the P(MMA–BA–AA) nanoparticles ranged from 50 to 70 nm, which was smaller than that of particles from macroemulsion polymerization.

FTIR spectrum analysis of P(MMA–BA–AA)

The FTIR spectrum of the P(MMA–BA–AA) polymer was measured, and the results are shown in Figure 2.

All of the peaks belonged to the characteristic peaks of the P(MMA–BA–AA) polymer. The peak around 3500 cm^{-1} were assigned to the —OH symmetric stretching vibrations from carboxyl group. The peak at 2952 cm^{-1} was the stretching vibrations of C—H. The peak at 1731 cm^{-1} was the characteristic absorption peak of carbonyl. The bands around 1147 cm^{-1} were assigned to C(O)—O stretching vibrations.

Characterization and analysis of the P(MMA–BA–AA)/PANI nanoparticles

Mechanism of the core–shell coating

The overall synthetic procedure of the P(MMA–BA–AA)/PANI core–shell complex particles is illustrated in Scheme 1.

First, aniline monomers were protonated onto positively charged anilinium ions in the presence of hydrochloric acid and were subsequently combined with negatively charged carboxyl groups of P(MMA–BA–AA). In other words, the aniline monomer could be attracted near the outer surface of the core particles. The polymerization of aniline was started under the action of APS. PANI-coated P(MMA–BA–AA) nanocomposite particles were prepared by *in situ* oxidative polymerization. The interaction between the P(MMA–BA–AA) core and PANI shell was enhanced obviously by the codoping of carboxyl groups in the interface of these core–shell particles. This was helpful in improving the stability and conductivity of the composite particles.

TEM analysis of P(MMA–BA–AA)/PANI

Figure 3 shows the TEM photographs of the P(MMA–BA–AA)/PANI core–shell particles. After PANI was coated onto the P(MMA–BA–AA) core nanoparticles, the core–shell structure of the particles could be clearly seen. Each particle had two color zones. The lighter one in the center area was the core polymer P(MMA–BA–AA). The darker part around the core polymer was PANI. As shown in Figure 3, a discontinuous PANI-shell layer was observed on the surfaces of the P(MMA–BA–AA) core particles [sample 2,

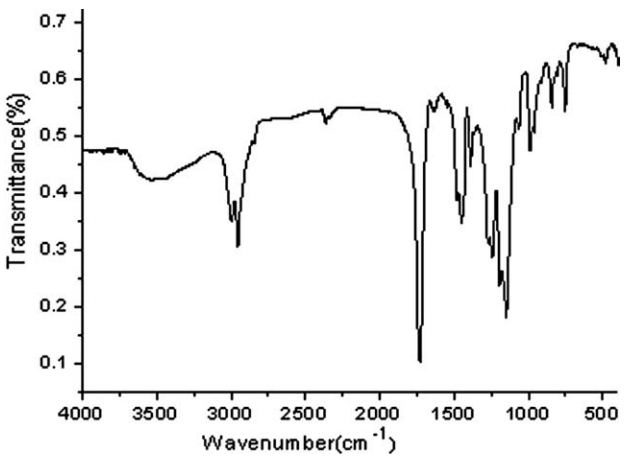

Figure 2 FTIR spectrum of P(MMA–BA–AA).

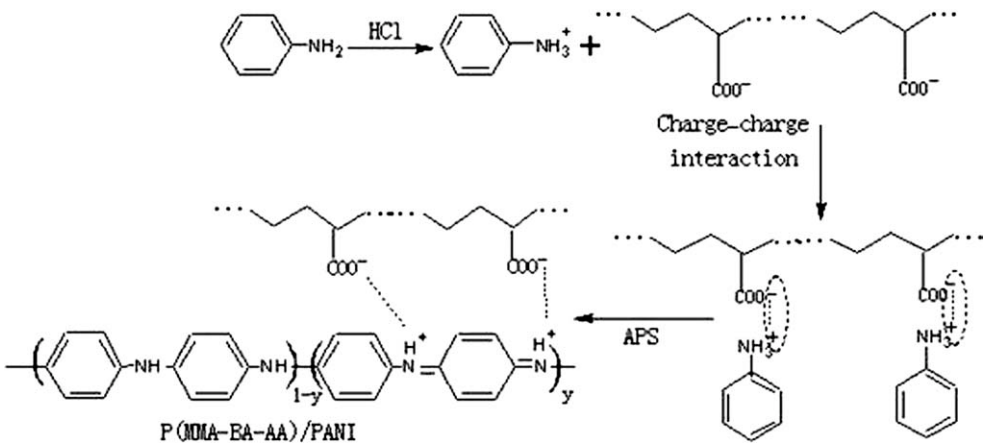

Scheme 1 Synthetic procedure for the production of P(MMA–BA–AA)/PANI core–shell complex particles.

Fig. 3(a,b)]. The thickness of the PANI shell ranged from 0 to 15 nm. The major reasons are explained. In the synthetic route, aniline was not sufficient to form a uniform shell coating over the core particles, and the growth of the PANI shell was guided by the interaction between —COOH of the core particles and —NH_2 of the aniline monomer. As the amount of aniline introduced was increased, PANI coated on the P(MMA–BA–AA) core became more uniform and thicker [sample 3, Fig. 3(c)]. The diameter of the P(MMA–BA–AA)/PANI composite nanoparticles ranged from 80 to 90 nm; this was larger than that of the P(MMA–BA–AA) core nanoparticles. However, when the amount of aniline reached 300 μL [sample 4, Fig. 3(d)], the chance of self-nucleation of aniline was high,[21] and P(MMA–BA–AA)/PANI composite particle coagulation occurred during the process of PANI synthesis. After the reaction was finished, some dark green granular substance precipitated on the bottom of the reactor. The agglomerates contained several P(MMA–BA–AA)/PANI composite nanoparticles. The core–shell structure of the particles could be still clearly seen. The diameter of the agglomerates was about 250 nm.

FTIR spectrum analysis of P(MMA–BA–AA)/PANI

The FTIR spectra of the P(MMA–BA–AA)/PANI particles are shown in Figure 4(a,b). The characteristic

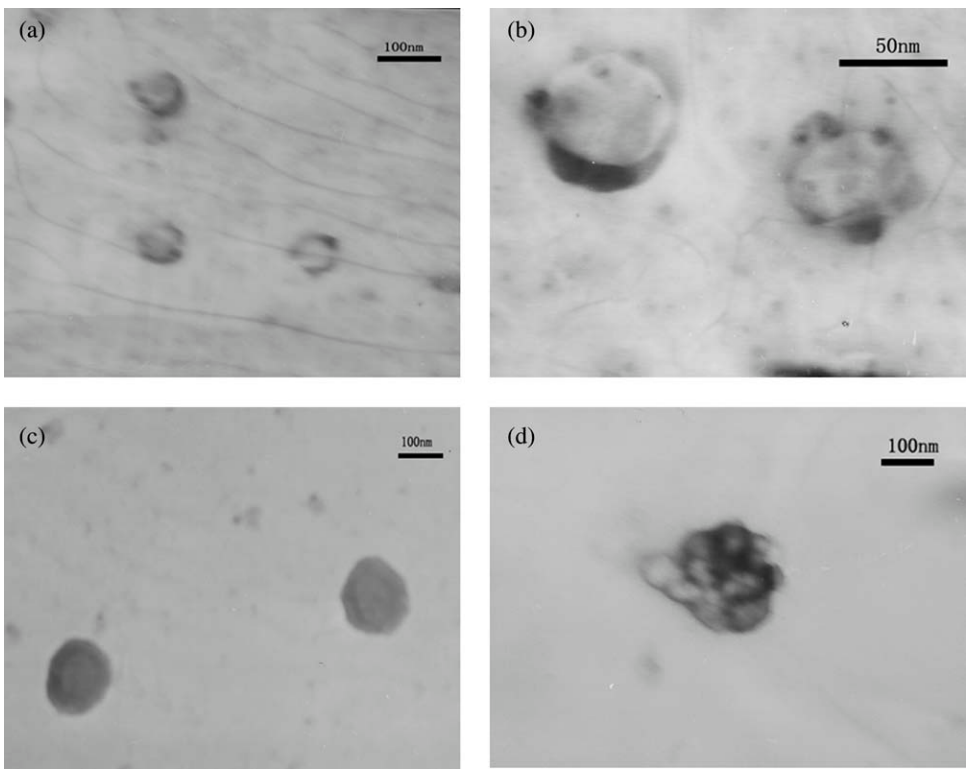

Figure 3 TEM photographs of samples (a,b) 2, (c) 3, and (d) 4.

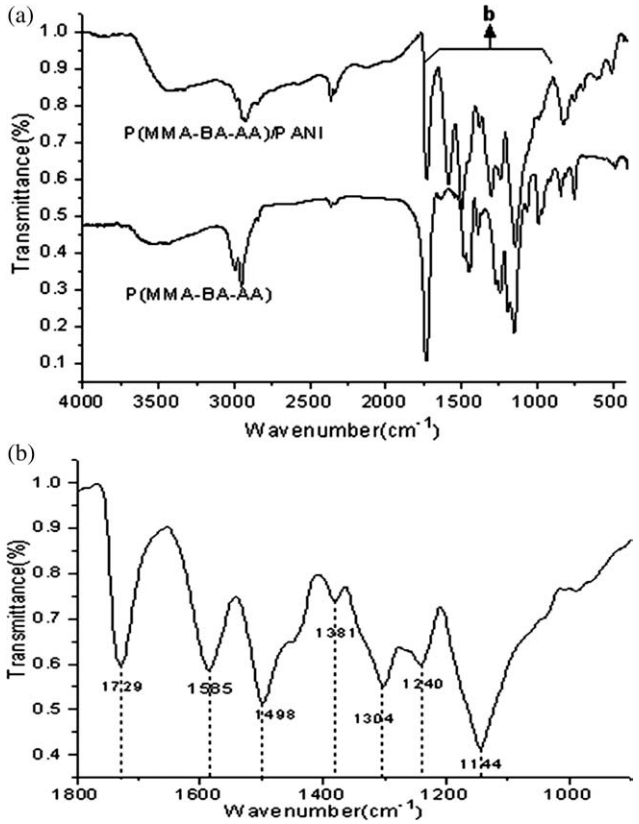

Figure 4 (a) FTIR spectrum of the P(MMA–BA–AA)/PANI particles and (b) a local enlargement of part a.

peaks of the P(MMA–BA–AA)/PANI particles around 1585 and 1498 cm^{-1} corresponded to the stretching of the quinone ring and benzene ring, respectively, of PANI. The band at 1304 cm^{-1} was the characteristic absorption peak of the C—N stretching vibrations of PANI. The aforementioned absorption peaks confirmed the existence of the PANI shell. All of this information indicated that the PANI was emeraldine rather than solely leucoemeraldine or pernigraniline. This structure is favored for the conductivity of the P(MMA–BA–AA)/PANI composite particles. At the same time, the characteristic absorption peaks of the P(MMA–BA–AA) core were observed. The peak at 2923 cm^{-1} was the stretching vibrations of C—H. The peak at 1730 cm^{-1} was the characteristic absorption peak of carbonyl, and the bands around 1145 cm^{-1} were assigned to the C(O)—O stretching vibrations. These absorption peaks were weaker than those of pure P(MMA–BA–AA) because the P(MMA–BA–AA) core was wrapped well in the PANI shell.

Ultraviolet–visible (UV–vis) spectra analysis of P(MMA–BA–AA)/PANI

A dedoped P(MMA–BA–AA)/PANI sample was obtained after sample 3 was washed with ammonia and ethanol. The UV–vis absorption spectrum of the dedoped P(MMA–BA–AA)/PANI is shown in Figure 5(b). The first absorption band, with a maximum at 326 nm, was assigned to the π–π* transition in the benzenoid structure, and the second band at 630 nm was ascribed to exciton formation in the quinonoid rings.

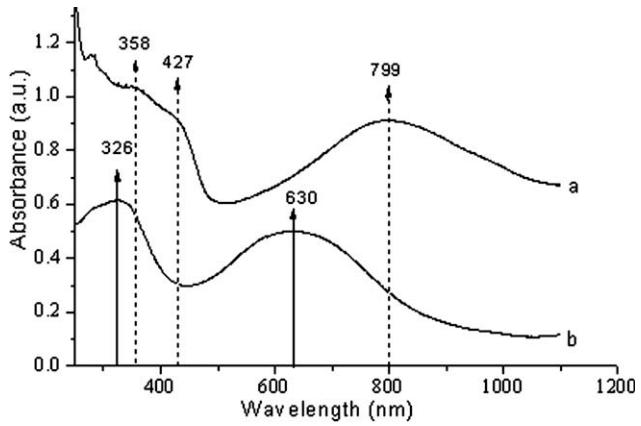

Figure 5 UV–vis spectra of the P(MMA–BA–AA)/PANI: (a) codoped with —COOH and HCl and (b) dedoped.

The dedoped PANI can be schematically represented by the following formula:

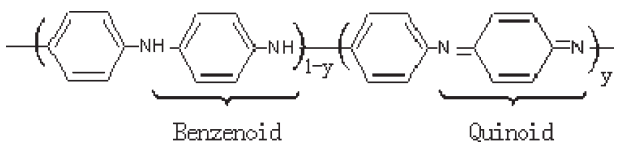

The UV–vis absorption spectrum of P(MMA–BA–AA)/PANI, which was codoped with —COOH of the P(MMA–BA–AA) core and hydrochloric acid, is shown in Figure 5(a). It shows that codoped PANI included three characteristic absorption bands observed at 358, 427, and 799 nm.[22,23] The first absorption band at 358 nm arose from electron transitions within the benzenoid segments. The second absorption band at 427 nm was found only at pH < 7 and represented the protonation stage of the PANI chains. The two bands around 358 and 427 nm were often combined into a flat or distorted single peak, which resulted in undefined sharpness. The absorption around 799 nm was assigned to the presence of a polaron resulting from the doping process. All of the information indicated that the P(MMA–BA–AA)/PANI sample contained conductive emeraldine. Through analysis, we know that the PANI shell was codoped with —COOH and HCl. That

TABLE II
Conductivity Values of the P(MMA–BA–AA)/PANI Core–Shell Latexes

Sample	Aniline (μL)	Conductivity (S/cm)
1	50	8×10^{-4}
2	100	0.11
3	200	2.05
4	300	2.01

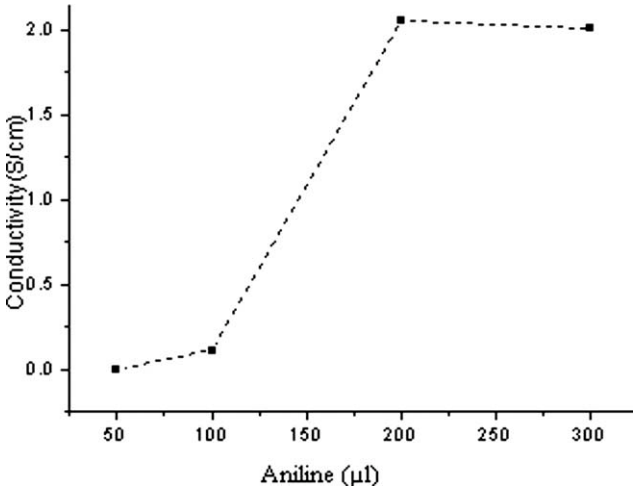

Figure 6 Conductivity of the P(MMA–BA–AA)/PANI core–shell latexes.

primarily corroborated the mechanism of core–shell coating.

Conductivities of the P(MMA–BA–AA)/PANI nanoparticles

The conductivity of the P(MMA–BA–AA)/PANI pellets was measured by a four-point probe. Every sample was measured three times. We took the average result of each sample as its conductivity. Table II and Figure 6 show the relationship between the added amount of aniline and the conductivity of the composite particles. From samples 1 to 3, the conductivity increased with increasing amount of aniline introduced; this was attributed to the more uniform and thicker PANI shell. We also observed a distinctive increase from samples 2 to 3. The maximum conductivity of 2.05 S/cm was observed in sample 3, which had a perfect core–shell structure. However, with 300 μL of aniline loaded, the self-nucleation of aniline existed and resulted in phase separation and a nonuniform shell coating. Therefore, the conductivity of sample 4 decreased slightly compared with that of sample 3.

CONCLUSIONS

A P(MMA–BA–AA) core latex with the size 50–70 nm was obtained by polymerization in a miniemulsion system with a redox initiator system consisting of sodium bisulfite (0.3 wt % on the basis of the monomer) and ammonium persulfate (0.2 wt % on the basis of the monomer) at 65°C. These P(MMA–BA–AA) nanoparticles prepared in the miniemulsion system were coated with a PANI layer by *in situ* polymerization (0°C). P(MMA–BA–AA)/PANI composites with a core–shell structure were successfully synthesized by the adjustment of the mass ratio of P(MMA–BA–AA) to aniline, and the optimum mass ratio was {m[P(MMA–BA–AA):m(aniline) = 0.31g:0.2 g]}. The core–shell structure of the P(MMA–BA–AA)/PANI composites was confirmed by TEM and FTIR spectroscopy. The UV–vis spectra showed that the PANI shell of the composite particles were codoped with —COOH inside and HCl outside. Furthermore, the electrical conductivities of the P(MMA–BA–AA)/PANI core–shell nanoparticles were studied. The experimental results show that sample 3, which had a perfect core–shell structure, possessed the highest conductivity of 2.05 S/cm.

References

1. Anand, J.; Palaniappan, S.; Sathyanarayana, D. N. Prog Polym Sci 1998, 23, 993.
2. Gurunathan, K.; Murugan, A. V.; Marimuthu, R.; Mulik, U. P.; Amalnerkar, D. P. Mater Chem Phys 1999, 61, 173.
3. da Silva, J. E. P.; de Torresi, S. I. C.; Torresi, R. M. Corros Sci 2005, 47, 811.
4. Jang, J.; Ha, J.; Cho, J. Adv Mater 2007, 19, 1772.
5. Wang, J. L.; Yang, W. Q.; Tong, P. C.; Lei, J. X. J Appl Polym Sci 2010, 115, 1886.
6. Kang, J. H.; Oh, Y. J.; Paek, S. M.; Hwang, S. J.; Choy J. H. Sol Energy Mater Solar Cells 2009, 93, 2040.
7. Shin, J. S.; Kim, J. H.; Cheong, I. W. Synth Met 2005, 151, 246.
8. Cho, Y. H.; Cho, M. S.; Choi, H. J.; Jhon, M. S. Colloid Polym Sci 2002, 280, 1062.
9. Ruckenstein, E.; Yang, S. Y. Synth Met 1993, 53, 283.
10. Okubo, M.; Fujii, S.; Minami, H. Colloid Polym Sci 2001, 279, 139.
11. Liu, Y. D.; Fang, F. F.; Choi, H. J. Langmuir 2010, 26, 12849.
12. Kim, S. G.; Lim, J. Y.; Sung, J. H.; Choi, H. J.; Seo, Y. Polymer 2007, 48, 6622.
13. Xu, X. J.; Chew, C. H.; Siow, K. S.; Wong, M. K.; Gan, L. M. Langmuir 1999, 15, 8067.
14. Anderson, C. D.; Sudol, E. D.; El-Aasser, M. S. Macromolecules 2002, 35, 574.
15. Asua, J. M. Prog Polym Sci 2002, 27, 1283.
16. Bechthold, N.; Tiarks, F.; Willert, M.; Landfester, K.; Antonietti, M. Macromol Symp 2000, 151, 549.
17. Bradley, M. A.; Prescott, S. W.; Schoonbrood, H. A. S.; Landfester, K.; Grieser, F. Macromolecules 2005, 38, 6346.
18. Stumbe, J. F.; Calderara, F.; Riess, G. Polym Bull 2001, 47, 277.
19. Shi, Y. C.; Wu, Y. S.; Hao, J. C.; Li, G. Z. J Polym Sci Part A: Polym Chem 2005, 43, 203.
20. Wang, Y.; Shi, Y. C.; Xu, X. K.; Liu, F.; Yao, H. L.; Zhai, G. Y. Colloids Surf A 2009, 345, 71.
21. Cho, M. S.; Cho, Y. H.; Choi, H. J.; Jhon, M. S. Langmuir 2003, 19, 5875.
22. Stejskal, J.; Kratochvil, P.; Radhakrishnan, N. Synth Met 1993, 61, 225.
23. Li, C. Y.; Chiu, W. Y.; Don, T. M. J Polym Sci Part A: Polym Chem 2007, 45, 3902.